Cardinal role of eukaryotic initiation factor 2 (eIF2α) in neuronal death : implication of PERK:IRE1α:ATF6 axis in Parkinson's pathology

Sonam Gupta[1] and Sarika Singh[1]

[1]CSIR-CDRI

May 5, 2020

Abstract

Background and purpose - In spite of decades research the etiology of Parkinson's disease (PD) is not yet well defined. The present study was conducted to assess the role of eukaryotic initiation factor 2 (eIF2α) in progressive dopaminergic neuronal death. Experimental approach - The investigation was done employing experimental rat model of parkinsonism and utilizing various interventions (YM08, 4μ8C, AEBSF, salubrinal, ursolic acid) of endoplasmic reticulum (ER) stress signaling. The mRNA and protein level of ER stress related signaling factors (GRP78, IRE1α, ATF6, eIF2α, ATF4, XBP-1, GADD153) were estimated along with various biochemical alterations (reactive oxygen species generation, levels of nitrite level, intracellular calcium, mitochondrial membrane potential), neuronal morphology and neuronal apoptosis after 3 and 7 day of experiment initiation. Key results - Findings with single administration of interventions showed that salubrinal exhibited significant protection against rotenone induced alterations in ER stress related signaling factors in comparison to other interventions. Therefore, further study was expanded with repeat dose of salubrinal. Rotenone administration in rat brain caused the dose dependent progressive neuronal death which was significantly attenuated with salubrinal treatment involving its diverse effects on altered levels of various ER stress related signaling factors and altered biochemical parameters. Conclusion and implications - Findings showed that rotenone administration induced PD pathology involve the dose dependent progressive neuronal death including various biochemical alterations with critical role of eukaryotic initiation factor 2α, suggesting the potential pharmacological utilization of salubrinal or salubrinal like molecule in therapeutics of Parkinson's diseases.

INTRODUCTION

The endoplasmic reticulum (ER), an organelle fundamentally requires to accomplish folding of newly translated proteins, for regulating their post-translational adaptations to achieve their anticipated physiological functions. Pathophysiological insults like redox imbalance, hypoxia, excessive protein synthesis, and altered calcium homeostasis perturb the ER functions, leading to the accretion of unfolded / misfolded proteins in the ER lumen, machinery depicted as ER stress (Mahdi et al., 2016), a mechanism known to activate a series of signals that comprise the unfolded protein response (UPR). The three major transducers of the UPR are located on ER membrane and named as PERK (PKR-like endoplasmic reticulum kinase), IRE1 (inositol-requiring 1), and ATF6 (activating transcription factor 6) (Shen et al ., 2002; Rutkowski and Kaufman., 2004). These three ER stress sensors palpate the occurrence of the unfolded proteins in the ER lumen and then communicate the signals to the nucleus and cytosol. Under physiological conditions all these three senors remain bound to ER chaperon glucose regulated protein 78 (GRP78) towards their ER-luminal domains and kept their activity suppresed (Shen et al., 2002). However, pathological conditions like accretion of unfolded/misfolded proteins in ER lumen, dissociates the chaperon-GRP78 from these ER membrane located sensors and allows their dimerization & activation. Dimerization and phosphorylation of PERK further phosphorylated the α-subunit of the eukaryotic initiation factor 2 (eIF2α), which further suppress

the protein synthesis to regulate the cellular protein load. In contrast to other signaling factors, ATF4 (activating transcription factor 4) eludes the phosphorylated eIF2α mediated translational attenuation due to the presence of upstream open reading frames (ORFs) at its 5'-untranslated region therefore, it could be stated that phosphorylation of eIF2α promotes the ATF4 translation. Initiation of ER stress also translocates the ATF6 to the golgi apparatus for its cleavage by S1P and S2P, and yield free cytoplasmic domain to act as a transcription factor. Activation of IRE1also catalyses the elimination of a small intron from mRNA of X-box-binding protein 1 (XBP1) thus makes a translational frameshift in XBP1 to generate an active transcription factor. Both activated ATF6 and XBP1 then bind to the ER stress response element and the UPR element, leading to the expression of intended genes (Walter and Ron, 2011). However, reports have shown that extreme ER stress may exhibit ER-dependent apoptosis by activation of GADD153 / CHOP (growth arrest DNA damage inducible gene 153 OR C/EBP homologous protein) and caspase-12 (Gao et al., 2013). The proapoptotic effects of GADD153 have also been observed initiated through increased reactive oxygen species (ROS) production. ER stress-mediated apoptosis is the third type of apoptosis signaling pathway that is independent of the membrane receptors or mitochondrial pathways and in this mechanism the upregulated GRP78 and XBP-1 expression are considered as ER stress markers (Wang et al., 2015). Previous studies from lab have suggested the involvement of ER stress in rotenone induced neuronal death however the detailed investigation for involvement of various ER stress related downstream signaling factors was remain to be done (Wu et al., 2014; Goswami et al., 2016). Xia et al. (2011) have also reported that interruption in ER function plays an significant role in neuronal pathology. With the scope of lacunae exist the present study was conducted in rotenone administered experimental rat model of parkinsonism and role of various signaling factors was evaluated. In order to our previous finding where we showed the prompt susceptibility of mid brain (MB) and striata (STR) for rotenone induced neuronal pathology the investigations of present study were done in these two brain regions (Swarnkar et al, 2010; 2011). Since we have reported the role of ER stress in rotenone induced neuronal death the inhibitors of various factors which may offer the neuroprotection were employed in study. To induce the neuronal death rotenone neurotoxin was employed in view of its significant implication in energy crisis and ER stress mediated neuronal apoptosis. Rotenone is a natural product extracted from the seeds and stems of several plants and primarily involve the impaired mitochondrial complex-I activity and depleted ATP level for neuronal death (Zhang et al., 2013). Studies from our lab and other's have showed the involvement of oxidative stress and nitrosative stress in rotenone administered rat brain in various rat brain regions (Khadrawy et al., 2017; Verma et al., 2018; Swarnkar et al., 2010). It has also been reported that rotenone administration in rat brain caused the altered behavioral, pathological and biochemical parameters (Swarnkar et al., 2010; 2011). Fernández et al. (2017) have also showed that involvement of reactive oxygen species, calcium and apoptosis in rotenone mediated neuronal death in rat brain.

MATERIALS AND METHODS

Experimental animals

The study was acquitted on male Sprague Dawley (SD) rats of body weight 180-200 gm, obtained from our division of laboratory animals, after approval from Institutional animal ethics committee. Rats were kept in polyacrylic cages with regular housing conditions, food and water was provided *ad libitum* .

Interventions employed

GRP-78 inhibitor, YM08 (5 mg/kg, Miyata et al., 2013) and ATF-6 inhibitor, AEBSF (10mg/kg, Jiang et al., 2011) were dissolved in normal saline separately and injected in tail vain of rat prior to 1 h of rotenone administration. While ATF-4 inhibitor, ursolic acid (25mg/kg, Ebert et al., 2015), IRE1 inhibitor, 4μ8C (5mg/kg, Ozlem Tufanli et al., 2017) and eIF2α inhibitor, salubrinal (1mg/kg, Wang et al., 2015) were dissolved in DMSO, injected via intraperitoneally route prior to 1 h of rotenone administration. The repeat dose of salubrinal was continued daily up to the day of sacrifice (3 and/or 7 day of rotenone administration).

Intranigral administration of rotenone by stereotaxy

Intranigral administration of rotenone (6μg or 12 μg) was done through stereotaxic surgery as reported in

Goswami et al (2016) and standard postoperative care was done. All experiments were repeated three to four times (n=3–4). The number of animals taken in each group per parameter was 6–8. Rats were categorized in seven groups named control, vehicle,*per se* (salubrinal treated), rotenone administered groups (6μg or 12μg) and rotenone + salubrinal treated group.

Subcellular fractionation for western blot

The subcellular cytosolic, nuclear and endoplasmic reticulum (ER) fractions were prepared according to the method described by Zong et al., (2003). In cytosolic fractions the level of GRP-78, eIF2α, p-eIF2α and cleaved caspase-12 were assessed while in nuclear fraction the protein XBP-1, ATF-4, ATF-6, GADD153 and cleaved caspase-3 were assessed. Proteins PERK, pPERK, IRE1α and pIRE1α were assessed in ER fraction. Protein was estimated by Lowry's method and identical concentration of protein was loaded in lanes for SDS-PAGE and proteins on gel were then transferred onto polyvinylidene difluoride membrane. Membranes were blocked with5% BSA solution for 2 h and separately incubated with primary antibodies like anti rabbit GRP-78, PERK, pPERK, ATF-4, eIF2α, p-eIF2α, pIRE1α, ATF-6, XBP-1, GADD 153, anti mouse caspase-12, caspase-3, β-actin and anti goat IRE1α overnight at 4^0C. After washing with PBS-T, the membranes were incubated with appropriate secondary antibodies conjugated with horseradish peroxidase for 2 h at room temperature. Signals were developed and visualized employing femtoLUCENT plus-HRP chemiluminescent substrate (G-biosciences, USA) and ChemiDoc HRS+ (Bio-Rad) respectively. Relative integrated density of obtained bands was estimated using Image J software and normalized by β-actin (Gupta et al., 2019).

mRNA expression by RT-PCR (Reverse Transcription Polymerase Chain reaction)

Total RNA was extracted from brain regions by trizol reagent based on the manufacturer guidelines and reported previously (Verma et al, 2018). The amplified PCR products were observed by electrophoresis using 2% agarose gel imaged by gel documentation system. Images were analyzed by software image J. Primer sequences, product length and Tm are given in Table 1.

Measurement of reactive oxygen species (ROS)

ROS level was estimated according to method described by Verma et al., (2018) and signals were recordede by fluorimeter (Varian Cary Eclipse, USA) at excitation of 485 nm and emission at 525 nm wavelengths.

Assessment of nitrite level

Nitrite level was estimated according to method described by Singh et al., (2010) and optical density of pink colored product was measured at 550 nm utilizing spectrophotometric microplate reader (Eon, Biotek, USA). Nitrite levels were reported in μM and extrapolated from standard curve of sodium nitrite.

Assessment of mitochondrial membrane potential (MMP)

The estimation of MMP was done as reported previously (Gupta et al, 2015) and the signals were measured using fluorescence spectrophotometer (Agilent, USA) at wavelength 508 nm excitation and 530 nm emission.

Measurement of intracellular calcium level

Estimation was done as reported previously (Biswas et al., 2018) employing fluo-3AM dye (5μM) and fluorescence intensity was measured using fluorescence spectrophotometer (Varian, Cary Eclipse) at 506 nm/530 nm excitation/emission.

Histology analysis

Tissue block preparation and sectioning and cresyl violet staining was done in brain section as reported previously (Goswami et al., 2015). Florojade C staining of brain sections were done to assess the degenerating neurons as reported previously (Biswas et al, 2018). Images were captured and analysed by Qwin V3 Software (Leica).

Comet assay

Comet assay was performed by previously described method (Gupta et al., 2014). The slides were stained with propidium iodide (40 µg / ml) to visualize the fragmented DNA and 60-70 images per slide were captured using fluorescent microscope (Nikon Eclipse TE2000-S).

Statistical analysis:

Data were represented as mean ± standard error of the mean (SEM). The alterations in various parameters were analyzed using one-way analysis of variance (ANOVA) post-hoc Newman-Keuls multiple comparisons test. Ap value of < 0.05 was taken as statistically significant.

RESULTS

Selection of intervention

Intervention was selected on the basis of protein levels of various signaling factors (Fig.1a-e). Firstly the experiment was conducted with single dose of intervention (YM08, AEBSF, Ursolic acid, 4µ8C and salubrinal) which was given to rats 1 h prior to rotenone (12µg) administration and protein level of signaling factors (GRP-78, p-PERK, dephosphorylation of eIF2α, ATF-4, p-IRE1-α, XBP-1, ATF-6, GADD 153, cleaved caspase12, cleaved caspase3) was estimated. Level of most of the above signaling factor was significantly altered after 7 days of rotenone administration with no per se effect of interventions. Rotenone administration caused the significant alteration in all estimated signaling factors however, diverse protection against rotenone induced altered level of signaling factors was observed with different interventions (Fig.1, Table 2 & 3). The level of PERK, IRE1 and eIF2α remain unchanged irrespective of treatment. Comparatively salubrinal treatment offered significant protection in the entire range of estimated factor in both studied rat brain regions though the extent of protection was varied for different factors (Table 2 & 3). Therefore, further the effect of repeat dose of salubrinal was evaluated in ER stress signaling / UPR in both rat brain regions.

Effect of salubrinal on rotenone induced altered mRNA levels of endoplasmic reticulum (ER) stress markers in both rat brain regions

mRNA level of GRP-78, GADD153, caspase-12 and caspase-3

Rotenone administration caused significantly increased mRNA levels of GRP-78, GADD153, caspase-12 and caspase-3 which was significantly inhibited with salubrinal treatment at both time points. Salubrinal treatment offered significant inhibition against rotenone induced increased mRNA levels (Fig. 2).

Effect of salubrinal on rotenone induced altered protein levels of endoplasmic reticulum (ER) stress markers in both rat brain regions

The ER stress related signaling factors like GRP-78, PERK, pPERK, IRE1α, pIRE1α, ATF-6, eIF2α, p-eIF2α, ATF-4, XBP-1, GADD 153 and cleaved caspase-12 were assessed in both MB and STR regions of rat brain after 3 days and 7 days of rotenone administration. The assessment was done in subcellular fractions as indicated in methodology section. Rotenone administration caused the increased level of GRP78, p-PERK, ATF4, p-IRE1, XBP-1, ATF6, GADD153, cleaved caspase12, cleaved caspase3 along with dephosphorylation of eIF2α. The level of PERK, IRE1 and eIF2α remain unaltered (Fig. 3).

Effect of salubrinal on rotenone induced biochemical alterations in both rat brain regions

Reactive oxygen species (ROS) generation

After 3 days of rotenone injection significantly increased ROS level was observed as compared to control however, after 7 days of rotenone administration no significant increase in ROS level was observed in both MB and STR regions as compared to control rat brain regions. Salubrinal per se treatment did not cause alteration in basal ROS level (Fig. 4a).

Nitrite level

Rotenone administration in rat brain caused significantly increased nitrite level in comparison to control in both MB and STR regions at both time point. Salubrinal *per se* treatment did not cause significant effect

on nitrite level in comparison to control levels in both studied brain regions. Salubrinal only injection had no significant effect on nitrite level (Fig. 4b).

Effect on Mitochondrial membrane potential (MMP)

Under physiological condition the maintenance of certain MMP is essential for the regulated synthesis of ATP, intracellular ion equilibrium and cellular death. In order to this, the assessment of MMP was done utilizing fluorescent dye rhodamine 123 after rotenone administration in both MB and STR region of rat brain A decline in the membrane potential was observed in both MB and STR region after 3and 7 days of rotenone administration in comparison to control. In salubrinal*per se* treated rat brain the MMP level was not altered and approximately identical to control values

(Fig. 4c).

Intracellular calcium level

Calcium encounter vital role in upholding of cellular functional equilibrium and mitochondrial activity therefore, its intracellular levels were estimated. Intracellular calcium level was found significantly increased in both MB and STR regions after 3 and 7 days of rotenone administration. Salubrinal treatment significantly attenuated the rotenone induced increased intracellular calcium level. Salubrinal only treatment did not exhibit significant effect on calcium level. (Fig. 4d).

Effect of salubrinal on rotenone induced altered neuronal morphology and degenerating neurons in both rat brain regions

Cresyl violet (CV) staining

Rotenone induced morphological alterations were assessed by cresyl violet (CV) staining of brain sections. Rotenone administration for 3 and 7 days exhibited the significant deterioration of neuronal nuclei in both mid brain and striata regions of rat brain (Fig. 5a). Salubrinal only treatment had no significant effect on neuronal nuclei in comparison to control. The analysis was done in terms of area and reported as μm^2.

Fluorojade C (FJ-C) staining

Fluorojade C is an anionic fluorescent dye and a marker of degenerating neurons. After 3 and 7 days of rotenone administration in rat brain significantly increased neuronal degeneration was observed in both MB and STR regions (Fig. 5b).Salubrinal only injection had no significant amendment in rat brain regions.

Effect of salubrinal on rotenone induced DNA fragmentation in both rat brain regions

After 3 and 7 days of rotenone administration considerable DNA fragmentation was observed in both MB and STR region of rat brain in comparison to control as assessed by comet assay (Fig. 5c). Salubrinal treatment offered considerable protection against rotenone induced increased DNA fragmentation. Salubrinal *per se* treatment did not cause significant effect on DNA fragmentation.

DISCUSSION

Present study was undertaken to evaluate the cardinally involved signaling factor among all ER stress related signaling factors and UPR like GRP78, transmembrane kinases - PERK & IRE1, ATF4 & 6, eIF2α, XBP-1, caspase 12 and GADD153. Since we intend to investigate the role of various signaling factor, the rats were exposed to rotenone which is highly toxic to neurons through its effect on mitochondrial complex-I activity and ER functionality as observed by us and others previously (Tong et al., 2016; Goswami et al, 2016; Gupta et al, 2019). To assess the effect of various signaling factors the rats were dosed with single bolus of various interventions of different factors. We have employed the intervention of GRP78 (YM08), IRE1 (4μ8C), ATF4 (Ursolic acid), ATF6 (AEBSF) and eIF2α (salubrinal) in study and estimated the protein levels of various factors (GRP-78, ATF-4, eIF2α, p-eIF2α, caspase-12, GADD 153, XBP-1, ATF-6, caspase-3, PERK, pPERK, IRE1α, pIRE1α) in different subcellular fractions. Findings indicated the diverse inhibitory effect of different interventions on various factors up to diverse extent. However, salubrinal treatment offered

comparatively panoptic protection against all of the rotenone induced altered ER stress and UPR related signaling factors, indicating the central role of eIF2α in rotenone induced neuronal death. Since salubrinal is a specific inhibitor of eIF2α phosphatase inhibitor enzyme, it prevents the dephosphorylation of eIF2α thus promoting the phosphorylated eIF2α. Phosphorylated eIF2α reduce the translation initiation and protects the cell against protein load and prevents the UPR. Since we have observed the protective effect of salubrinal against rotenone induced altered level of various ER stress signaling factors/ UPR we further aimed to explore the possibility of pharmacological use of salubrinal in PD therapeutics. Number of evidences suggested that ER stress is plebeian pathological hallmark of PD as evident in experimental models of disease (Colla et al., 2012). ER stress markers have also been reported in the substantia nigra pars compacta region of human post-mortems brain of sporadic PD patients (Slodzinski et al., 2009). Observations showed the immunoreactivity of the UPR related markers like pPERK and peIF2α in neuromelanin containing dopaminergic neurons in the substantia nigra of PD cases, suggesting their critical role in disease pathology. In addition, pPERK immunoreactivity is also co-localized with augmented immunoreactive α-synuclein dopaminergic neurons reflecting the alliance of UPR commencement with the accumulation and α-synuclein aggregation. Therefore, rotenone was employed in study which induces the PD like pathology and energy crisis along with ER stress (Swarnkar et al, 2010, 2011; Gupta et al, 2019; Jagmag et al, 2016). The study was designed to investigate the time and dose dependent effect of rotenone on neuronal viability, biochemical alterations and how salubrinal executed its effect on rotenone induced adverse conditions. To attain this aim the rotenone was administered in rat brain and rats were sacrificed at 3rd and 7th day of rotenone administration as detailed in methodology section.

Firstly we assess the mRNA level of key ER stress related factor GRP78, GADD153, caspase12 and caspase3 after 3 and 7 day of treatment. Findings showed that rotenone administration in rat brain caused the significantly increased expression levels of GRP78, GADD153, caspase 12 and neuronal death in both dose and time dependent manner which were inhibited with salubrinal treatment at both time points. The protein level of various factors (GRP-78, ATF-4, eIF2α, p-eIF2α, caspase-12, GADD 153, XBP-1, ATF-6, caspase-3, PERK, pPERK, IRE1α, pIRE1) was also estimated in both MB and STR regions in subcellular fractions. In this context we have observed the rotenone induced significantly increased level of GRP78, pPERK, pIRE1, ATF4, XBP1, ATF6, GADD153, caspase12, depleted level of peIF2α along with neuronal death in both time and dose dependent manner. In order to this observation recent finding by Ramalingam et al, (2019) showed that rotenone caused the mitochondrial dysfunction, ER stress and affected mitochondria-associated ER contacts and consequent dopaminergic neuronal death. Reports also showed the rotenone induced increased transcriptional level of GRP78, GADD153 and caspase3 along with increased translational level of GRP78, XBP1, GADD153 and caspase3 in rat brain (Ma et al, 2019; Peng et al, 2018). A study in LUHMES monoculture showed that rotenone causes the increased level of ATF4 and oxidative stress which could be prevented with thiol mediated stress responses of astrocytes to protect the neurons (Gutbier et al, 2018). Study in PC12 cells and experimental rats showed that rotenone caused the PERK phosphorylation and subsequent activation of ATF4 and GADD153 to induce the neuronal death (Wu et al, 2014). Tong et al. (2016) have also reported that rotenone noticeably induced the neuronal-apoptosis along with caspase-12 activation in the substantia nigra pars compacta (SNpc). In agreement to our findings the previous studies have also demonstrated that caspase-3 could be activated by ER stress related marker caspase-12 (Katayama et al., 2004). In concordance to observed salubrinal induced protection against rotenone induced neuronal death Sokka et al. (2007) have also shown that salubrinal could offer the inhibition in kainic acid induced neuronal death in rat brain.

Observed ER stress reflects the altered balance of ER lumen and may involve the other pathological incidents like oxidative stress and affected mitochondrial activity. Since ER is the major intracellular calcium reservoir, its stressed conditions reflects the affected calcium homeostasis. Such high level of calcium are required for various calcium dependent chaperon for proper protein folding in ER (Sano and Reed, 2013; Krebs et al, 2015). ER stress induced altered clearing of protein will lead to an accretion of misfolded proteins in ER lumen which could induce the calcium efflux through ER (Deniaud et al., 2008) and subsequent increased calcium influx in mitochondria, collectively inducing the changes in mitochondrial pH and ROS production

(Smaili et al., 2009). Previous studies from our lab and others have also showed the involvement of calcium in rotenone mediated neuronal death (Swarnkar et al., 2012; Fernandez et al., 2017).

In view of these reports we have estimated the level of intracellular calcium level. Rotenone administration caused the significantly increased level of calcium in dose dependent manner which were significantly attenuated with salubrinal treatment in both MB and STR regions. Such ER-lumen released calcium may concentrate in the matrix of the mitochondria and may offer the mitochondrial depolarization, disrupt the mitochondrial electron transport and increased ROS production (Görlach et al, 2006). Other authors have also reported the rotenone induced increased ROS production (Wang et al., 2018) which further disrupt the mitochondrial membrane potential to trigger cytochrome c release, which foster the activation of caspase-9 to initiate the mitochondrial-targeted apoptotic signals (Chunxin et al., 2009).

Therefore, further we have estimated the mitochondrial membrane potential (MMP) and ROS generation in both MB and STR regions after rotenone / rotenone+salubrinal treatment. Rotenone administration caused the acute (observed after 3 day) significant increase in ROS level and mitochondrial depolarization however the chronic (after 7 day) treatment did not exhibit the significant increase in ROS level and mitochondrial depolarization though the levels were high in comparison to respective control rat brain regions. Such acute increase in ROS may further increase the calcium release from ER lumen through sensitization of ER calcium-release channels and cause the protein misfolding and direct the cell towards death. The depleted MMP was observed after acute treatment (after 3 day of rotenone administration) however the chronic (after 7 day) treatment showed the depleted MMP but it was not significantly different from the respective control rat brain regions. The depleted MMP also suggested the release of various proapoptotic factors from mitochondria which may subsequent promote the neuronal death (Rego et al, 2001). Previously we have observed the role of nitrite in rotenone induced neuronal death which could be attenuated with salubrinal in neuro2A cells (Gupta et al, 2019) therefore we have also estimated the level of nitrite in both MB and STR regions. Rotenone administration caused significantly increased level of nitrite in both concentration and time dependent manner which was significantly inhibited with salubrinal treatment in both studied rat brain regions. Such increased level of nitric oxide / nitrite and ROS may further react to each other to generate the more toxic reactive species peroxynitrite which affect the mitochondrial functions as well as caused the permanent damage in DNA (Ramdial et al., 2017)

Along with these biochemical alterations the neuronal morphology, degenerating neurons and DNA fragmentation was also assessed in both MB and STR regions. The neuronal morphology was assessed by cresyl violet staining of the rat brain sections (Ludvig et al., 2008). Rotenone administration to rat brain caused the significant altered neuronal morphology in both MB and STR regions which was attenuated with salubrinal treatment. Further the degenerating neurons were observed by florojade staining. Rotenone administration caused the degeneration of neurons at both concentrations of rotenone in both studied brain regions. Rotenone induced degeneration of neurons was significantly attenuated with salubrinal treatment. Further to assess the effect of rotenone on genetic material the comet assay was performed. Rotenone administration caused significant DNA fragmentation in both regions which was attenuated with salubrinal treatment. In conclusions, findings suggested the key role of eIF2α in rotenone induced adverse effects in rat brain MB and STR. Salubrinal treatment exhibited the significant protection of neurons against rotenone induced ER stress and UPR signaling mediated DNA fragmentation and neuronal apoptosis involving biochemical parameters like ROS generation, nitrite level, restored mitochondrial membrane potential and intracellular calcium levels.

Acknowledgement

Author Sonam Gupta is thankful to the Indian Council of Medical Research (ICMR), India, for senior research fellowship and Academy of Scientific and Innovative Research (AcSIR) for providing opportunity to conduct research at CSIR-CDRI. Authors are also thankful to funding agency Science and Engineering Research Board for providing financial support (EMR/2015/001282).

Conflict of interest

Authors have no conflict of interest.

REFERENCES

1. Mahdi AA, Rizvi SH, Parveen A. Role of Endoplasmic Reticulum Stress and Unfolded Protein Responses in Health and Diseases. Indian J Clin Biochem. 2016; 2:127-37.
2. Shen J, Chen X, Hendershot L, Prywes R. ER stress regulation of ATF6 localization by dissociation of BiP/GRP78 binding and unmasking of Golgi localization signals. Dev Cell. 2002; 3: 99–111.
3. Rutkowski DT, Kaufman RJ. A trip to the ER: coping with stress. Trends Cell Biol. 2004; 1:20-8.
4. Walter P, Ron D. The unfolded protein response: from stress pathway to homeostatic regulation. Science. 2011; 334: 1081-1086.
5. Gao B, Zhang XY, Han R, Zhang TT, Chen C, Qin ZH, et al. The endoplasmic reticulum stress inhibitor salubrinal inhibits the activation of autophagy and neuroprotection induced by brain ischemic preconditioning. Acta Pharmacol Sin. 2013; 34:657–66.
6. Wang T, Zhang SJ, Cao SL, Guo WZ, Yan B, Fang HB. Protective effects of salubrinal on liver injury in rat models of brain death. Chin Med J (Engl). 2015;11:1523-8.
7. Wu L, Luo N, Zhao HR, Gao Q, Lu J, Pan Y, Shi JP, Tian YY, Zhang YD. Salubrinal protects against rotenone-induced SH-SY5Y cell death via ATF4-parkin pathway. Brain Res. 2014; 1549: 52–62.
8. Goswami P, Gupta S, Biswas J, Sharma S, Singh S. Endoplasmic reticulum stress instigates the rotenone induced oxidative apoptotic neuronal death: a study in rat brain, Molecular neurobiology. 2016; 8: 5384-400.
9. Xia Q, Feng X, Huang H, Du L, Yang X, Wang K. Gadolinium-induced oxidative stress triggers endoplasmic reticulum stress in rat cortical neurons. J Neurochem. 2011; 117:38-47.
10. Swarnkar S, Singh S, Mathur R, Patro IK, Nath C. A study to correlate rotenone induced biochemical changes and cerebral damage in brain areas with neuromuscular coordination in rats. Toxicology. 2010; 272: 17-22.
11. Swarnkar S, Singh S, Sharma S, Mathur R, Patro IK, Nath C. Rotenone induced neurotoxicity in rat brain areas: a histopathological study. Neurosci Lett. 2011;501: 123-7.
12. Zhang X, Yan H, Yuan Y, Gao J, Shen Z, Cheng Y. Cerebral ischemia-reperfusion-induced autophagy protects against neuronal injury by mitochondrial clearance. Autophagy. 2013; 9:1321–33.
13. Khadrawy YA, Salem AM, El-Shamy KA, Ahmed EK, Fadl NN, Hosny EN. Neuroprotective and Therapeutic Effect of Caffeine on the Rat Model of Parkinson's disease Induced by Rotenone. J Diet Suppl. 2017; 5:553-572.
14. Verma D, Gupta S, Biswas J, Joshi N, Singh a, Gupta P, Tiwari S, Raju S, Chaturvedi S, Wahajuddin M, and Singh S. New therapeutic activity of metabolic enhancer Piracetam in treatment of neurodegenerative disease: participation of caspase independent death factors, oxidative stress, inflammatory responses and apoptosis. BBA Molecular Basis of Disease . 2018; 1864, 2078-2096.
15. Fernández - Moriano C, González-Burgos E, Iglesias I, Lozano R, Gómez-Serranillos MP. Evaluation of the adaptogenic potential exerted by ginsenosides Rb1 and Rg1 against oxidative stress-mediated neurotoxicity in an in vitro neuronal model. PLoSOne. 2017; 8:e0182933.
16. Miyata Y, Li X, Lee HF, Jinwal UK, Srinivasan SR, Seguin SP, Young ZT, Brodsky JL, Dickey CA, Sun D, Gestwicki JE. Synthesis and initial evaluation of YM-08, a blood-brain barrier permeable derivative of the heat shock protein 70 (Hsp70) inhibitor MKT-077, which reduces tau levels. ACS Chem Neurosci. 2013;6:930-9.
17. Jiang YH, Shi Y, He YP, Du J, Li RS, Shi HJ, Sun ZG, Wang J. Serine protease inhibitor 4-(2-aminoethyl)benzenesulfonyl fluoride hydrochloride (AEBSF) inhibits the rat embryo implantation in vivo and interferes with cell adhesion in vitro. Contraception. 2011;6:642-8.
18. Ebert SM, Dyle MC, Bullard SA, Dierdorff JM, Murry DJ, Fox DK, Bongers KS, Lira VA, Meyerholz DK, Talley JJ, Adams CM. Identification and Small Molecule Inhibition of an Activating Transcription Factor 4 (ATF4)-dependent Pathway to Age-related Skeletal Muscle Weakness and Atrophy. J Biol Chem. 2015 ;42:25497-511.
19. Tufanli O, Telkoparan Akillilar P, Acosta-Alvear D, Kocaturk B, Onat UI, Hamid SM, Çimen I, Walter P, Weber C, Erbay E. Targeting IRE1 with small molecules counteracts progression of atherosclerosis. Proc Natl Acad Sci U S A. 2017 ;8:E1395-E1404.

20. Paxinos G, Watson C. The Rat Brain in Sterotaxic Coordinates. Academic Press, New York. 1998; 1 –120.
21. Zong WX, Li C, Hatzivassiliou G, Lindsten T, Yu QC, Yuan J, Thompson CB. Bax and Bak can localize to the endoplasmic reticulum to initiate apoptosis. J Cell Biol. 2003; 7: 59-69.
22. Gupta S, Biswas J, Gupta P, Singh A, Tiwari S, Mishra A, Singh S. Salubrinal attenuates nitric oxide mediated PERK:IRE1α: ATF-6 signaling and DNA damage in neuronal cells.

Neurochem Int. 2019;131:104581.

1. Sarika S, Kumar S, Dikshit M. Involvement of mitochondrial apoptoticpathway and nitric oxide synthase in 6-hydroxydopamine and lipopolysacchride induced dopaminergic neuronal death. Redox Rep. 2010; 15: 1–8.
2. Gupta S, Goswami P, Biswas J, Joshi N, Sharma S, Nath C, Singh S. 6-Hydroxydopamine and lipopolysaccharides induced DNA damage in astrocytes: involvement of nitric oxide and mitochondria. Mutat Res Genet Toxicol Environ Mutagen. 2015; 778: 22-36.
3. Biswas J, Gupta S, Verma D, Gupta P, Singh A, Tiwari S, Goswami P, Sharma S, Singh S. Involvement of glucose related energy crisis and endoplasmic reticulum stress: Insinuation of streptozotocin induced Alzheimer's like pathology. Cellular signaling. 2018; 42: 211-226.
4. Ohmura A, Nakajima W, Ishida A, Yasuoka N, Kawamura M, Miura S, Takada G. Prolonged hypothermia protects neonatal rat brain against hypoxic-ischemiaby reducing both apoptosis and necrosis. Brain Dev. 2005; 27:517-526.
5. Gupta S, Verma DK, Biswas J, Rama Raju KS, Joshi N, Wahajuddin M, Singh S. The metabolic enhancer piracetam attenuates mitochondrion-specific endonuclease G translocation and oxidative DNA fragmentation. Free Radic Biol Med. 2014; 73: 278-290.
6. Lowry OH, Rosebrough NJ, Farr AI, Randall RJ. Protein measurement with the Folin phenol reagent. J Biol Chem. 1951; 193: 265–275.
7. Tong Q, Wu L, Gao Q, Ou Z, Zhu D, Zhang Y. PPARβ/δ Agonist Provides Neuroprotection by Suppression of IRE1α-Caspase-12-Mediated Endoplasmic Reticulum Stress Pathway in the Rotenone Rat Model of Parkinson's Disease. Mol Neurobiol. 2016; 6:3822-3831.
8. Colla E, Coune P, Liu Y, Pletnikova O, Troncoso JC, Iwatsubo T, Schneider BL, Lee MK. Endoplasmic reticulum stress is important for the manifestations of α-synucleinopathy in vivo. J Neurosci. 2012; 32:3306-3320.
9. Slodzinski H, Moran LB, Michael GJ, Wang B, Novoselov S, Cheetham ME, Pearce RK, Graeber MB. Homocysteine-induced endoplasmic reticulum protein (herp) is up-regulated in Parkinsonian substantia nigra and present in the core of Lewy bodies. Clin. Neuropathol. 2009; 28: 333–343.
10. Jagmag SA, Tripathi N, Shukla SD, Maiti S, Khurana S. Evaluation of Models of Parkinson's Disease. Front Neurosci. 2016; 19:9-503.
11. Ramalingam M, Huh YJ, Lee YI. The Impairments of α-Synuclein and Mechanistic Target of Rapamycin in Rotenone-Induced SH-SY5Y Cells and Mice Model of Parkinson's Disease. Front Neurosci. 2019;13:1028.
12. Ma J, Yuan L, Wang SJ, Lei J, Wang Y, Li YN, Yu BL. Electroacupuncture improved locomotor function by regulating expression of tyrosine hydroxylase and α-synuclein proteins and transcription activating factor 6 and transcription factor X box binding protein 1 mRNAs in substantia nigra of rats with Parkinson's disease.[Article in Chinese] Zhen Ci Yan Jiu. 2019;11:805-9.
13. Peng T, Liu X, Wang J, Liu Y, Fu Z, Ma X, Li J, Sun G, Ji Y, Lu J, Wan W, Lu H. Fluoxetine-mediated inhibition of endoplasmic reticulum stress is involved in the neuroprotective effects of Parkinson's disease. Aging (Albany NY). 2018; 12:4188-4196.
14. Gutbier S, Spreng AS, Delp J, Schildknecht S, Karreman C, Suciu I, Brunner T, Groettrup M, Leist M. Prevention of neuronal apoptosis by astrocytes through thiol-mediated stress response modulation and accelerated recovery from proteotoxic stress. Cell Death Differ. 2018 12:2101-2117.
15. Katayama T, Imaizumi K, Manabe T, Hitomi J, Kudo T, Tohyama M. Induction of neuronal death by ER stress in Alzheimer's disease. J Chem Neuroanat. 2004; 28:67-78.

16. Sokka AL, Putkonen N, Mudo G, Pryazhnikov E, Reijonen S, Khiroug L, Belluardo N, Lindholm D, Korhonen L. Endoplasmic reticulum stress inhibition protects against excitotoxic neuronal injury in the rat brain. J Neurosci 2007; 27:901-908.
17. Sano R, Reed JC. ER stress-induced cell death mechanisms. Biochim Biophys Acta. 2013; 12:3460-3470.
18. Krebs J, Agellon LB, Michalak M. Ca(2+) homeostasis and endoplasmic reticulum (ER) stress: An integrated view of calcium signaling. Biochem Biophys Res Commun. 2015;1:114-21.
19. Calì T, Ottolini D, Brini M Mitochondria, calcium, and endoplasmic reticulum stress in Parkinson's disease. Biofactors. 2011; 3:228-40.
20. Deniaud A, Sharaf el dein O, Maillier E, Poncet D, Kroemer G, Lemaire C, Brenner C. Endoplasmic reticulum stress induces calcium-dependent permeability transition, mitochondrial outer membrane permeabilization and apoptosis. Oncogene. 2008; 27:285-299.
21. Smaili S, Hirata H, Ureshino R, Monteforte PT, Morales AP, Muler ML, Terashima J, Oseki K, Rosenstock TR, Lopes GS, Bincoletto C. Calcium and cell death signaling in neurodegeneration and aging. An Acad Bras Cienc. 2009; 81:467- 475.
22. Swarnkar Supriya, Goswami Poonam, Kamat Pradeep Kumar, Gupta Sonam, Patro Ishan K., Singh Sarika, Nath Chandishwar.. Rotenone-induced apoptosis and role of calcium: a study on Neuro-2a cells. Arch Toxicol. 2012; 86, 1387- 1397.
23. Görlach A, Klappa P, Kietzmann T. The endoplasmic reticulum: folding, calcium homeostasis, signaling, and redox control. Antioxid Redox Signal. 2006; 8:1391-418.
24. Wang H, Dong X, Liu Z, Zhu S, Liu H, Fan W, Hu Y, Hu T, Yu Y, Li Y, Liu T, Xie C, Gao Q, Li G, Zhang J, Ding Z, Sun J .Resveratrol Suppresses Rotenone-induced Neurotoxicity Through Activation of SIRT1/Akt1 Signaling Pathway. Anat Rec (Hoboken). 2018; 6:1115-1125.
25. Chunxin Wang and Richard J. Youle. The Role of Mitochondria in Apoptosis. Annu Rev Genet. 2009; 43: 95–118.
26. RegoAC, VesceS, NichollsDG.The mechanism of mitochondrial membrane potential retention following release of cytochrome c in apoptotic GT1-7 neural cells. Cell Death Differ. 2001; 10:995-1003.
27. Ramdial K, Franco MC, Estevez AG. Cellularmechanismsof peroxynitriteinduced neuro nal death. Brain Res Bull. 2017;133 :4-11.
28. Ludvig N, Sheffield LG, Tang HM, Baptiste SL, Devinsky O, Kuzniecky RI. Histological evidence for drug diffusion across the cerebral meninges into the underlying neocortex in rats. Brain Res. 2008; 1188:228–232.

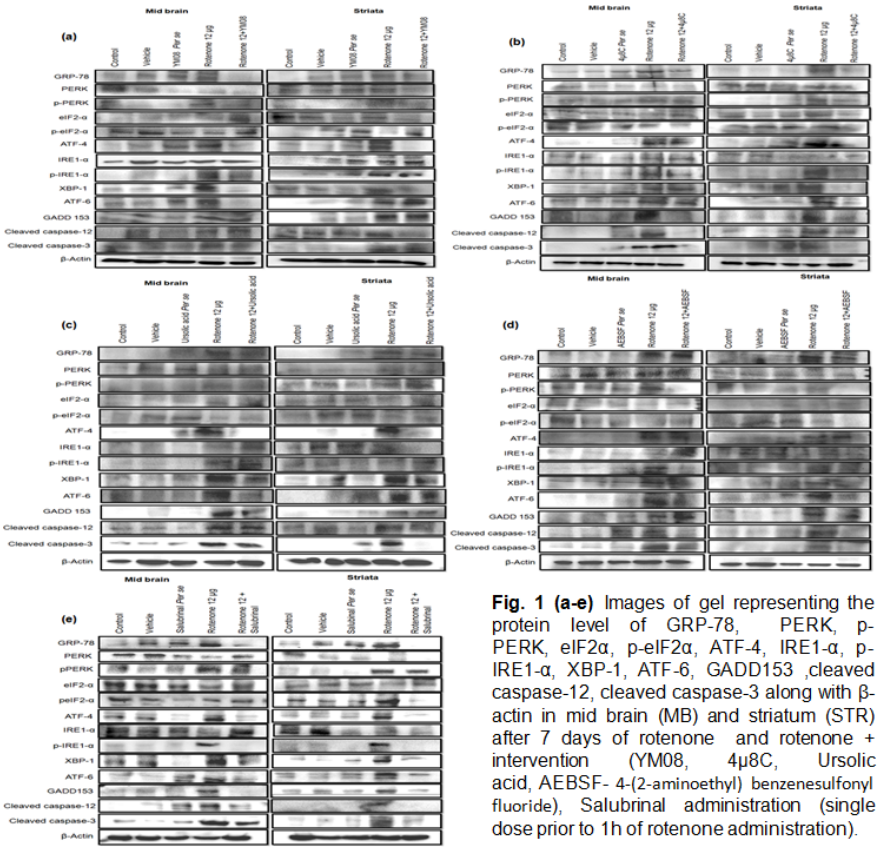

Fig. 1 (a-e) Images of gel representing the protein level of GRP-78, PERK, p-PERK, eIF2α, p-eIF2α, ATF-4, IRE1-α, p-IRE1-α, XBP-1, ATF-6, GADD153 ,cleaved caspase-12, cleaved caspase-3 along with β-actin in mid brain (MB) and striatum (STR) after 7 days of rotenone and rotenone + intervention (YM08, 4μ8C, Ursolic acid, AEBSF- 4-(2-aminoethyl) benzenesulfonyl fluoride), Salubrinal administration (single dose prior to 1h of rotenone administration).

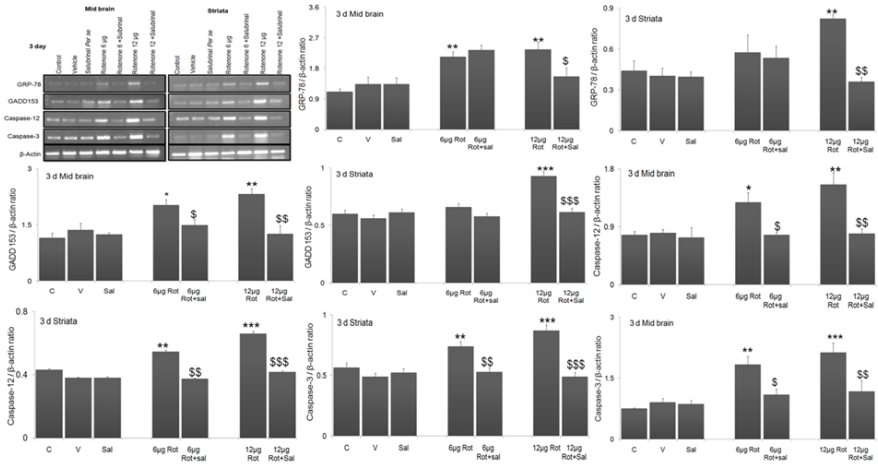

Fig. 2 (a) Images of gel representing the mRNA level of GRP-78, GADD153, caspase-12, caspase-3 along with β-actin in mid brain (MB) and striatum (STR) regions of rat brain after 3 days of rotenone administration. Graphs showing the quantification of observed mRNA level with respect to loading control β-actin in MB and STR regions of rat brain. Data are expressed as mean±SEM and analyzed by ANOVA post hoc Newman-Keuls multiple comparison test. *=p<0.05, **=p<0.01, ***=p<0.001 (Control vs. Rotenone treated). $=p<0.05, $$=p<0.01, $$$=p<0.001 (Rotenone treated vs Rotenone+Salubrinal treated). (C=control, V=vehicle, Sal=salubrinal, Rot=rotenone, Rot+Sal=rotenone+salubrinal).

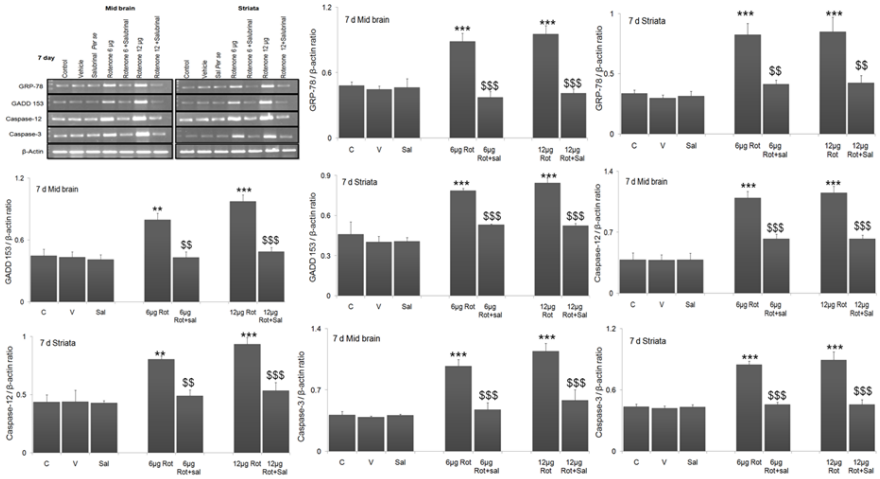

Fig. 2 (b) Images of gel representing the mRNA level of GRP-78, GADD153, Caspase-12 and caspase-3 along with β-actin in mid brain (MB) and striatum (STR) regions of rat brain after 7 days of rotenone administration. Graphs illustrating the quantification of observed mRNA level with respect to loading control β-actin in MB and STR regions of rat brain. Data are expressed as mean ± SEM and analyzed by ANOVA post hoc Newman-Keuls multiple comparison test. **=p<0.01, ***=p<0.001 (Control vs. Rotenone treated). $$=p<0.01, $$$=p<0.001 (Rotenone treated vs Rotenone + Salubrinal treated). (C=control, V=vehicle, Sal=salubrinal, Rot=rotenone, Rot+Sal=rotenone+salubrinal.

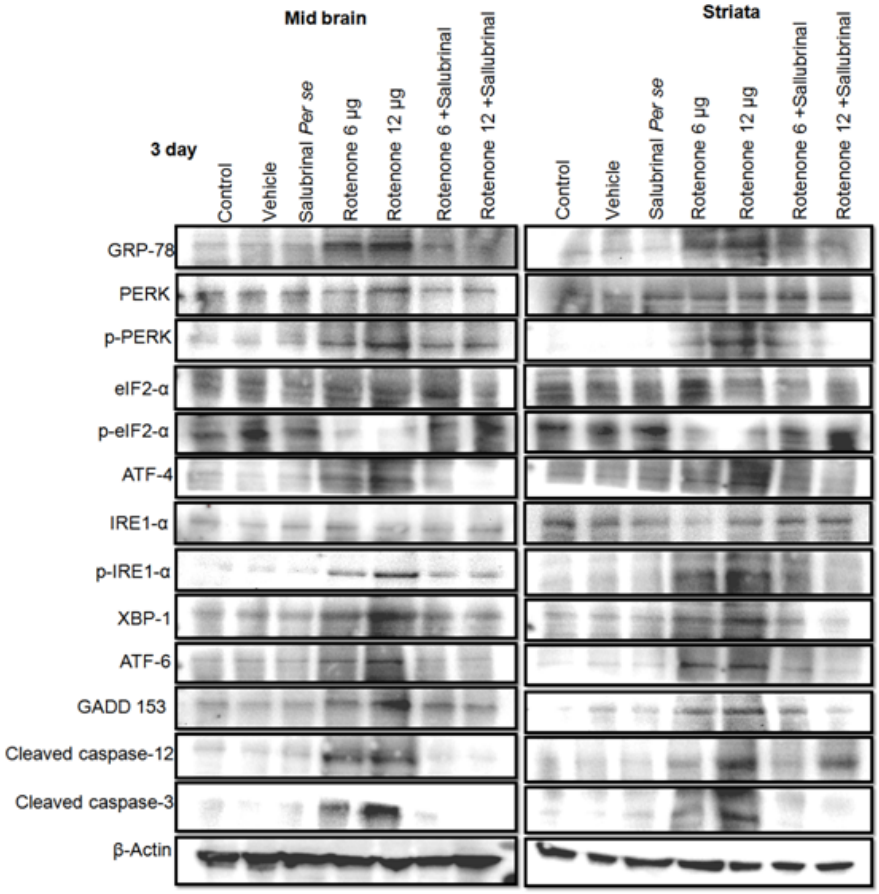

Fig. 3 (a) Images of gel representing the protein level of GRP-78, PERK, p-PERK, eIF2α, p-eIF2α, ATF-4, IRE1-α, p-IRE1-α, XBP-1, ATF-6, GADD153, cleaved caspase-12, cleaved caspase-3 along with β-actin in mid brain (MB) and striatum (STR) after 3 days of rotenone administration.

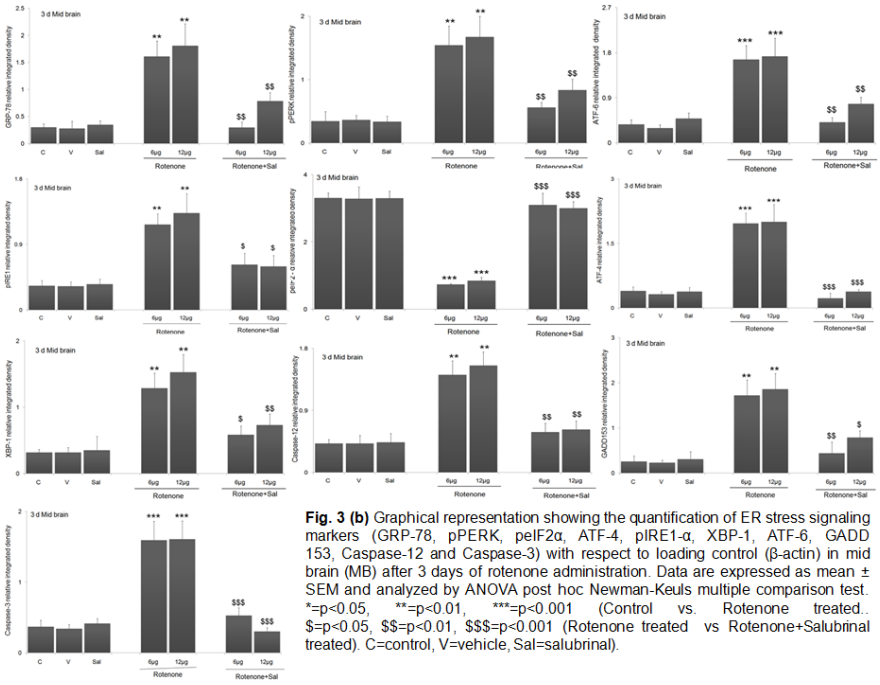

Fig. 3 (b) Graphical representation showing the quantification of ER stress signaling markers (GRP-78, pPERK, peIF2α, ATF-4, pIRE1-α, XBP-1, ATF-6, GADD 153, Caspase-12 and Caspase-3) with respect to loading control (β-actin) in mid brain (MB) after 3 days of rotenone administration. Data are expressed as mean ± SEM and analyzed by ANOVA post hoc Newman-Keuls multiple comparison test. *=p<0.05, **=p<0.01, ***=p<0.001 (Control vs. Rotenone treated.. $=p<0.05, $$=p<0.01, $$$=p<0.001 (Rotenone treated vs Rotenone+Salubrinal treated). C=control, V=vehicle, Sal=salubrinal).

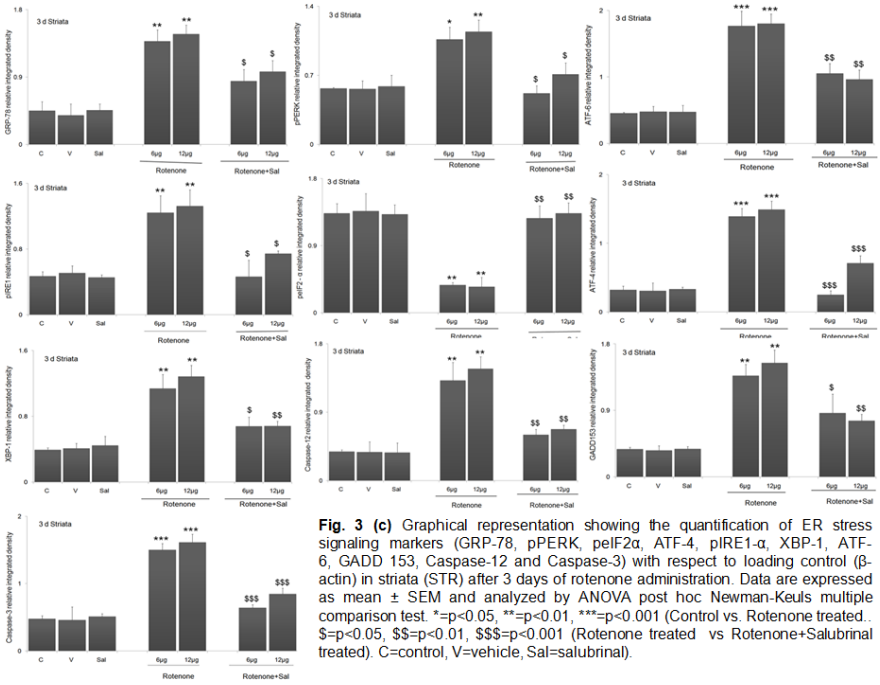

Fig. 3 (c) Graphical representation showing the quantification of ER stress signaling markers (GRP-78, pPERK, peIF2α, ATF-4, pIRE1-α, XBP-1, ATF-6, GADD 153, Caspase-12 and Caspase-3) with respect to loading control (β-actin) in striata (STR) after 3 days of rotenone administration. Data are expressed as mean ± SEM and analyzed by ANOVA post hoc Newman-Keuls multiple comparison test. *=p<0.05, **=p<0.01, ***=p<0.001 (Control vs. Rotenone treated.. $=p<0.05, $$=p<0.01, $$$=p<0.001 (Rotenone treated vs Rotenone+Salubrinal treated). C=control, V=vehicle, Sal=salubrinal).

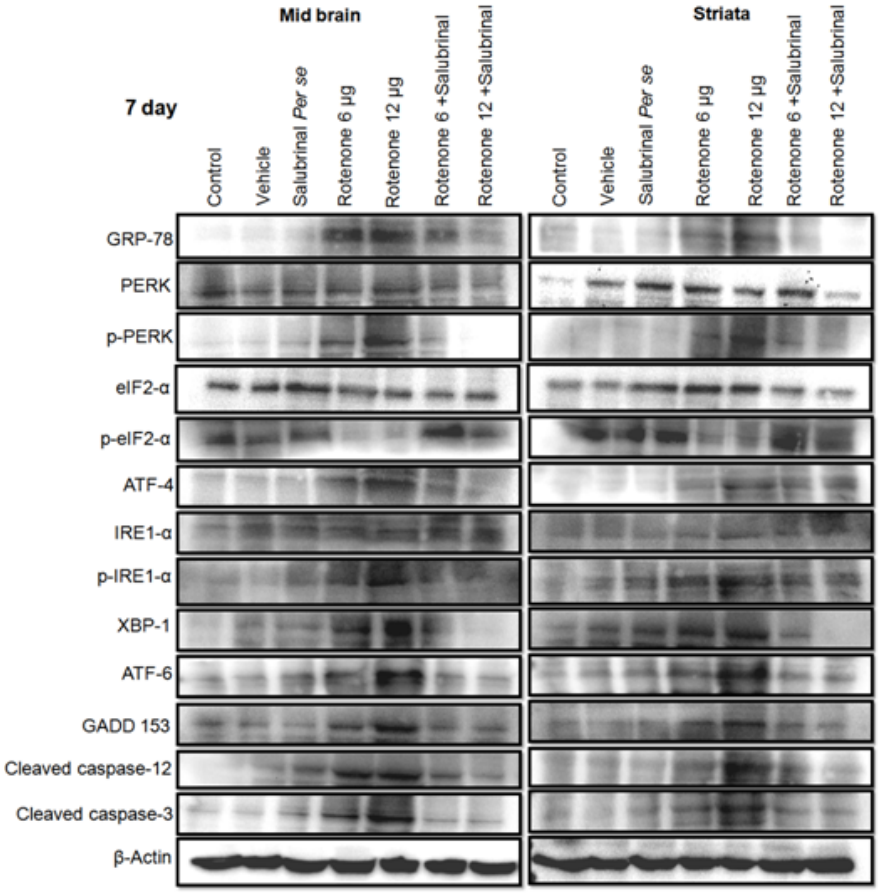

Fig. 3 (d) Images of gel representing the protein level of GRP-78, PERK, p-PERK, eIF2α, p-eIF2α, ATF-4, IRE1-α, p-IRE1-α, XBP-1, ATF-6, GADD 153, cleaved caspase-12, cleaved caspase-3 along with β-actin in mid brain (MB) and striatum (STR) after 7 days of rotenone administration.

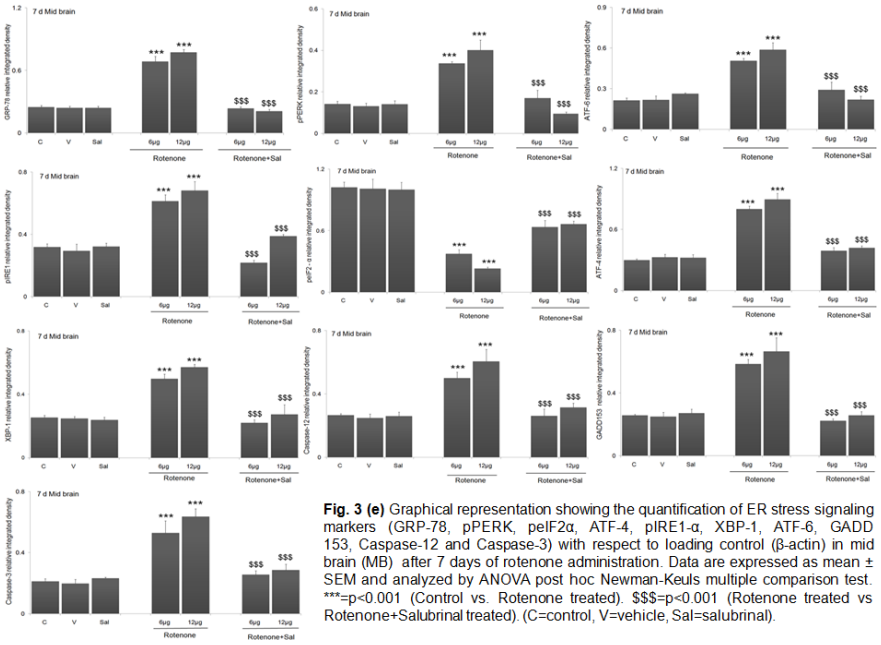

Fig. 3 (e) Graphical representation showing the quantification of ER stress signaling markers (GRP-78, pPERK, peIF2α, ATF-4, pIRE1-α, XBP-1, ATF-6, GADD 153, Caspase-12 and Caspase-3) with respect to loading control (β-actin) in mid brain (MB) after 7 days of rotenone administration. Data are expressed as mean ± SEM and analyzed by ANOVA post hoc Newman-Keuls multiple comparison test. ***=p<0.001 (Control vs. Rotenone treated). $$$=p<0.001 (Rotenone treated vs Rotenone+Salubrinal treated). (C=control, V=vehicle, Sal=salubrinal).

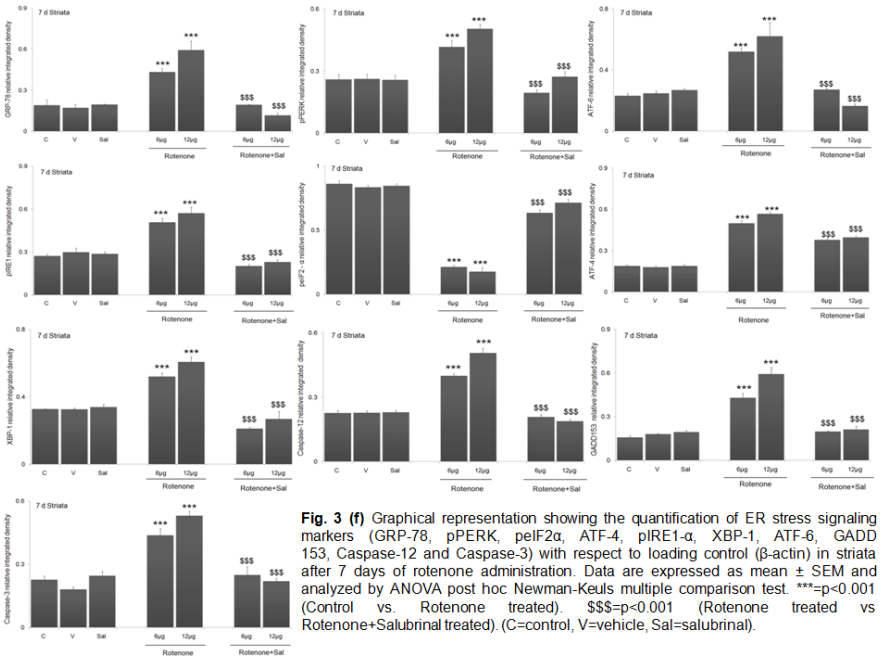

Fig. 3 (f) Graphical representation showing the quantification of ER stress signaling markers (GRP-78, pPERK, peIF2α, ATF-4, pIRE1-α, XBP-1, ATF-6, GADD 153, Caspase-12 and Caspase-3) with respect to loading control (β-actin) in striata after 7 days of rotenone administration. Data are expressed as mean ± SEM and analyzed by ANOVA post hoc Newman-Keuls multiple comparison test. ***=p<0.001 (Control vs. Rotenone treated). $$$=p<0.001 (Rotenone treated vs Rotenone+Salubrinal treated). (C=control, V=vehicle, Sal=salubrinal).

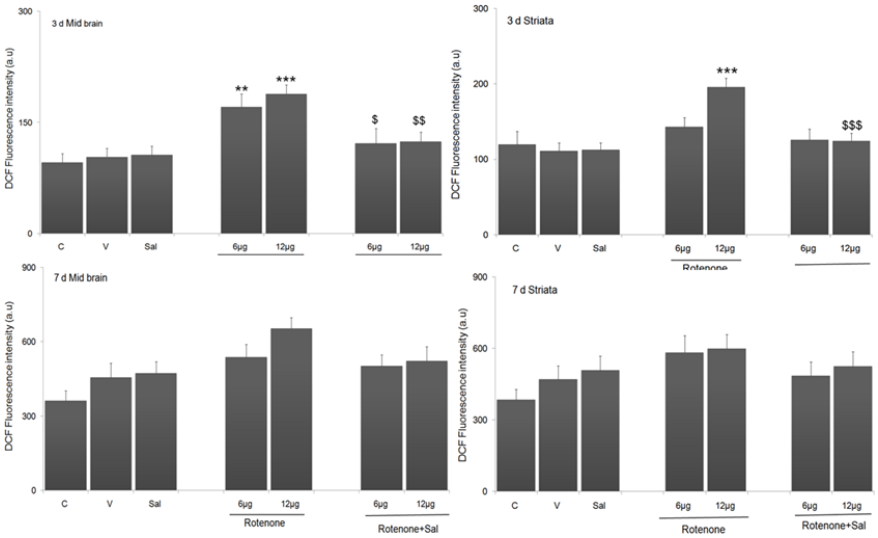

Fig. 4 (a) Bar diagram illustrating the ROS generation in mid brain (MB) and striata (STR) regions after 3 & 7 days of rotenone administration. Data are expressed as mean ± SEM and analyzed by ANOVA post hoc Newman-Keuls multiple comparison test. **=p<0.01,***=p<0.001 (Control vs. Rotenone treated). $=p<0.05, $$=p<0.01, $$$=p<0.001 (Rotenone treated vs Rotenone+Salubrinal treated). (C=control, V=vehicle, Sal=salubrinal).

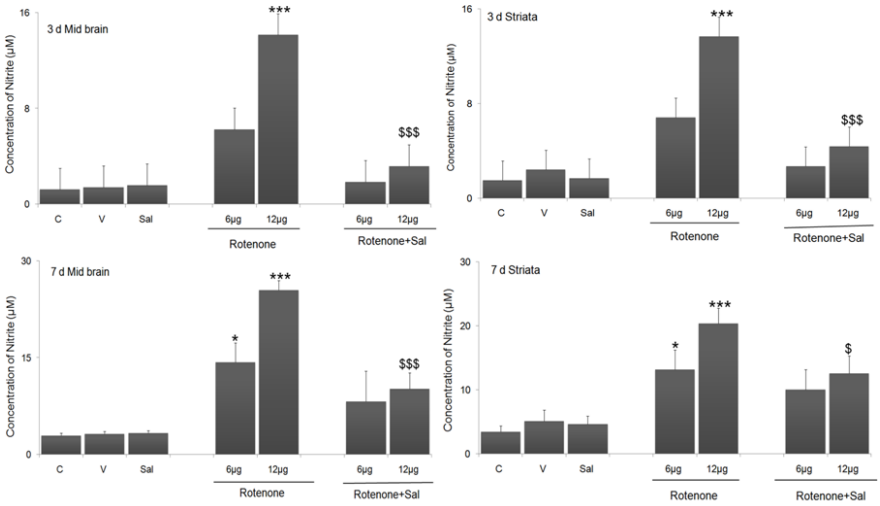

Fig. 4 (b) Bar diagram showing the nitrite level in mid brain (MB) and striata (STR) regions after 3 & 7 days of rotenone administration. Data are expressed as mean ± SEM and analyzed by ANOVA post hoc Newman-Keuls multiple comparison test. *=p<0.05,***=p<0.001 (Control vs. Rotenone treated). $=p<0.05, $$$=p<0.001 (Rotenone treated vs Rotenone+Salubrinal treated). (C=control, V=vehicle, Sal=salubrinal).

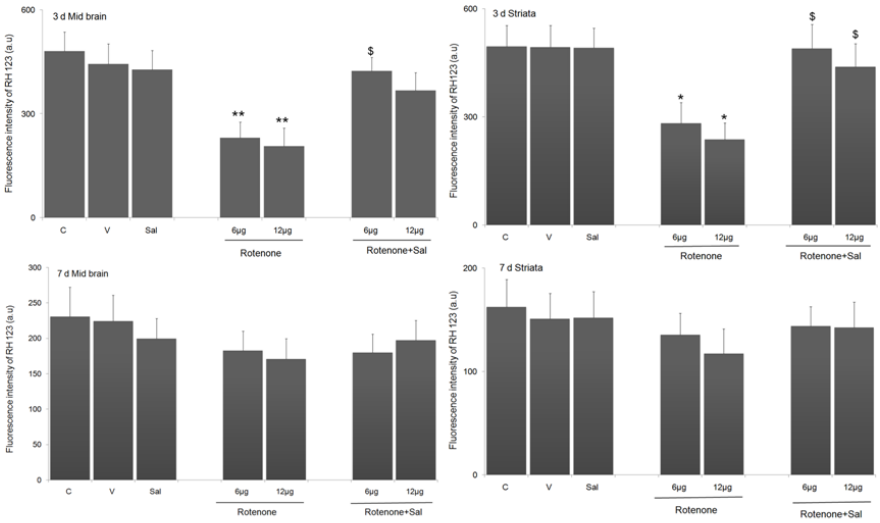

Fig. 4 (c) Graphical representation of mitochondrial membrane potential (MMP) in mid brain (MB) and striatum (STR) after 3 & 7 days of rotenone administration. (Abbreviations c=control, v=vehicle, sal=salubrinal). Data are expressed as mean ± SEM and analyzed by ANOVA post hoc Newman-Keuls multiple comparison test. *=p<0.05,**=p<0.01 (Control vs. Rotenone treated). $=p<0.05(Rotenone treated vs Rotenone+Salubrinal treated).

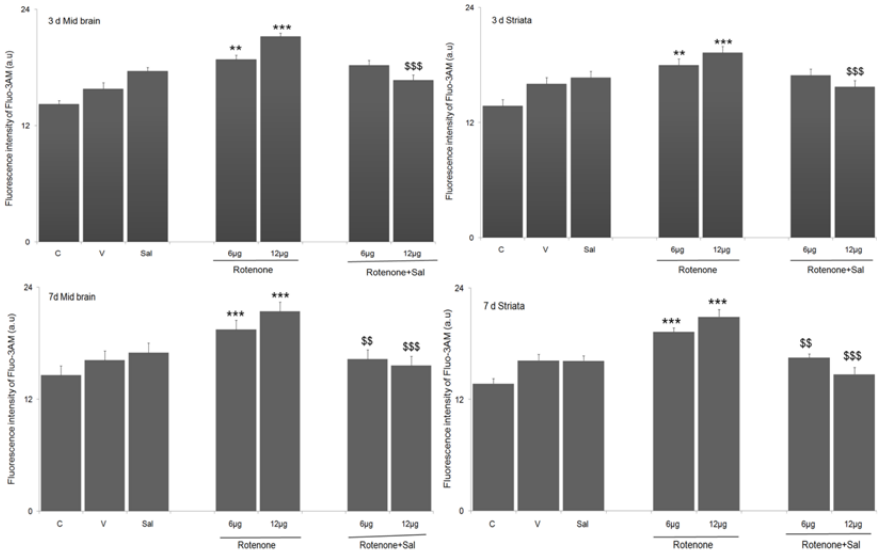

Fig. 4 (d) Bar diagram illustrating the intracellular calcium level in mid brain (MB) and striatum (STR) after 3 & 7 days of rotenone administration. (Abbreviations c=control, v=vehicle, sal=salubrinal). Data are expressed as mean±SEM and analyzed by ANOVA post hoc Newman-Keuls multiple comparison test. **=p<0.01, ***=p<0.001 (Control vs. Rotenone treated). $$=p<0.01, $$$=p<0.001 (Rotenone treated vs Rotenone+Salubrinal treated).

Hosted file

primer table 1 Jan 2020.docx available at https://authorea.com/users/304333/articles/434736-cardinal-role-of-eukaryotic-initiation-factor-2-eif2%CE%B1-in-neuronal-death-implication-of-perk-ire1%CE%B1-atf6-axis-in-parkinson-s-pathology

Hosted file

Table 3 Striata.docx available at https://authorea.com/users/304333/articles/434736-cardinal-role-of-eukaryotic-initiation-factor-2-eif2%CE%B1-in-neuronal-death-implication-of-perk-ire1%CE%B1-atf6-axis-in-parkinson-s-pathology

Hosted file

Table 2 Mid brain.docx available at https://authorea.com/users/304333/articles/434736-cardinal-role-of-eukaryotic-initiation-factor-2-eif2%CE%B1-in-neuronal-death-implication-of-perk-ire1%CE%B1-atf6-axis-in-parkinson-s-pathology

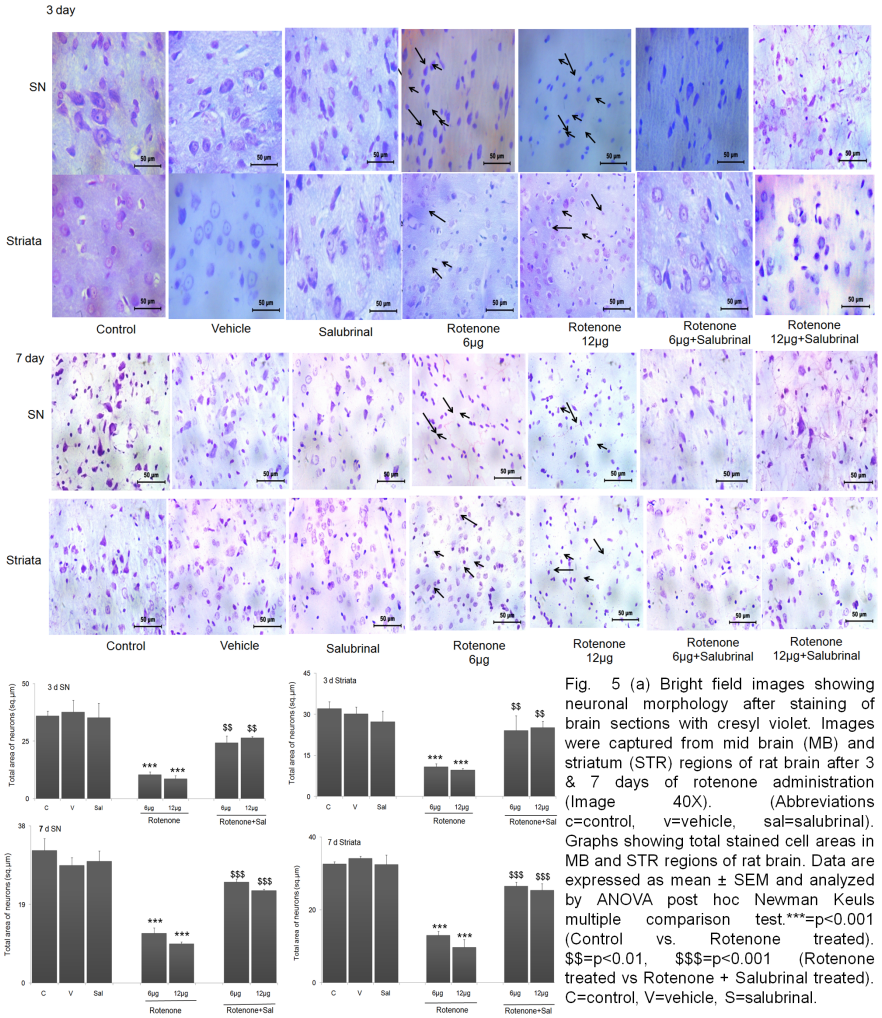

Fig. 5 (a) Bright field images showing neuronal morphology after staining of brain sections with cresyl violet. Images were captured from mid brain (MB) and striatum (STR) regions of rat brain after 3 & 7 days of rotenone administration (Image 40X). (Abbreviations c=control, v=vehicle, sal=salubrinal). Graphs showing total stained cell areas in MB and STR regions of rat brain. Data are expressed as mean ± SEM and analyzed by ANOVA post hoc Newman Keuls multiple comparison test.***=p<0.001 (Control vs. Rotenone treated). $$=p<0.01, $$$=p<0.001 (Rotenone treated vs Rotenone + Salubrinal treated). C=control, V=vehicle, S=salubrinal.

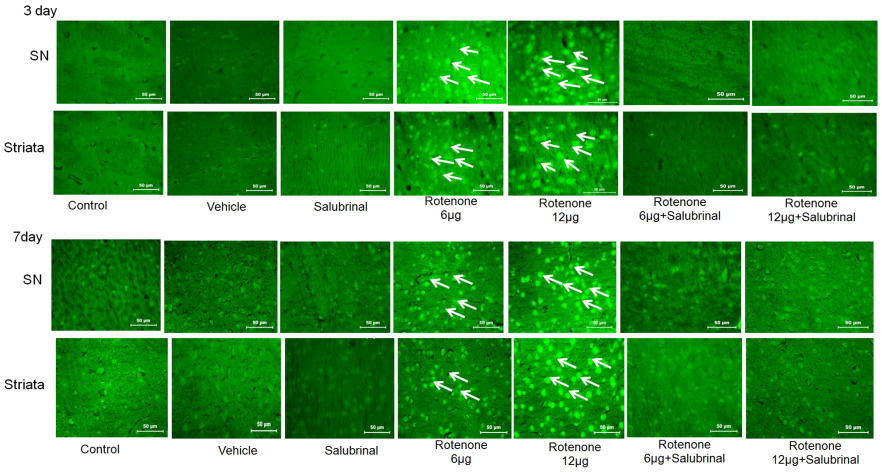

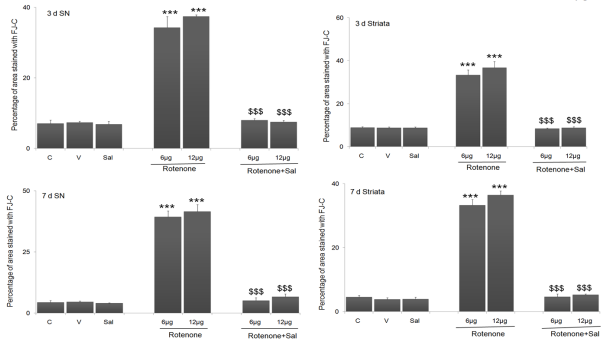

Fig. 5 (b) Fluorescent images showing degenerated neurons stained by fluorojade C in substantia nigra (SN) and striatum (STR) regions of rat brain after 3 & 7 days of rotenone administration (Image 40X). Graphs showing fluorojade C stained area in SN and STR regions of rat brain. Data are expressed as mean ± SEM and analyzed by ANOVA post hoc Newman Keuls multiple comparison test. ***=p<0.001 (Control vs. Rotenone treated). $$$=p<0.001 (Rotenone treated vs Rotenone + Salubrinal treated). Abbreviations C=control, V=vehicle, Sal=salubrinal.

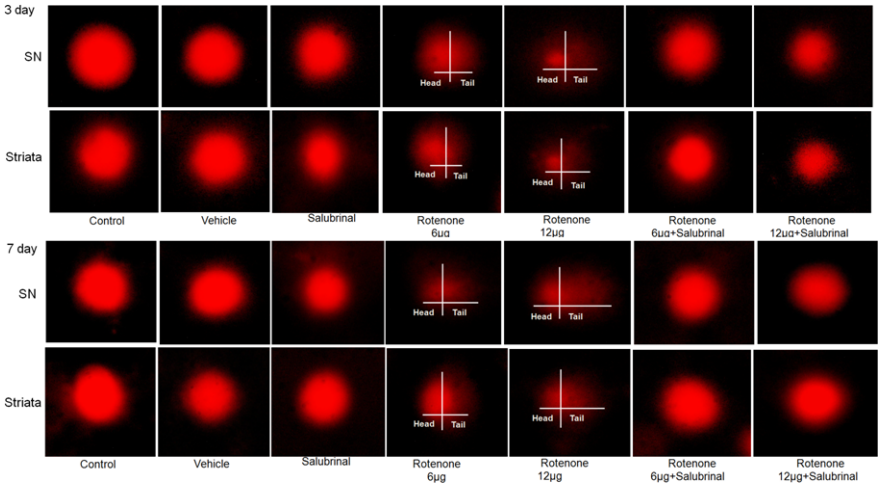

Fig. 5 (c) Fluorescent images showing DNA fragmentation in mid brain (MB) and striatum (STR) regions of rat brain after 3 and 7 days of rotenone administration. Rorenone administration caused the DNA fragmentation as reflected by comet tail which was inhibited with salubrinal treatment considerably.